

# Acetazolamide-mediated carbonic anhydrase inhibition suppresses human peripheral blood mononuclear cell proliferation via G1/S cell cycle arrest

Syazili Mustofa<sup>1\*</sup> , Mohamad Sadikin<sup>2</sup> , Sarmoko<sup>3</sup> 

<sup>1</sup>Department of Biochemistry, Molecular Biology, and Physiology Faculty of Medicine, Universitas Lampung, Bandar Lampung, Indonesia.

<sup>2</sup>Department of Biochemistry and Molecular Biology, Faculty of Medicine, Universitas Indonesia, Jakarta, Indonesia.

<sup>3</sup>Department of Pharmacy, Faculty of Science, Institut Teknologi Sumatera, Indonesia

\*Corresponding author: Jl. Prof. Dr. Ir. Sumantri Brojonegoro, No. 01, Bandar Lampung 35141. Email: [syazilimustofa.dr@gmail.com](mailto:syazilimustofa.dr@gmail.com)

## ABSTRACT

**Background:** Carbonic anhydrase (CA) regulates intracellular  $\text{CO}_2/\text{HCO}_3^-$  homeostasis and supplies carboxyl donors for the sixth step of *de novo* purine biosynthesis. Disruption of this step is predicted to impair nucleotide pool accumulation and arrest cell cycle progression.

**Objective:** This study investigated whether CA inhibition by acetazolamide suppresses T lymphocyte proliferation.

**Methods:** Human peripheral blood mononuclear cells (PBMCs) were stimulated with phytohemagglutinin (PHA, 1% v/v) or interleukin-2 (IL-2, 10 ng/mL). Acetazolamide was applied at 6.25–50  $\mu\text{M}$ . Cell viability, DNA synthesis, and cell cycle distribution were assessed using WST-1 assay, BrdU incorporation, and propidium iodide flow cytometry, respectively.

**Results:** Acetazolamide reduced PBMC viability and DNA synthesis dose-dependently in both PHA- and IL-2-stimulated cultures ( $p < 0.05$ ). IL-2-stimulated cells showed greater sensitivity, with significant inhibition at 12.5  $\mu\text{M}$  versus 25  $\mu\text{M}$  for PHA-stimulated cells. Flow cytometry revealed G1/S arrest in all treated groups: S phase decreased from 8.52% to 3.82% (PHA) and from 1.27% to 0% (IL-2) at 50  $\mu\text{M}$ , with G2/M uniformly suppressed to  $\leq 0.57\%$ .

**Conclusion:** Acetazolamide suppresses PBMC proliferation through G1/S arrest, consistent with CA inhibition depleting  $\text{CO}_2/\text{HCO}_3^-$ -dependent carboxyl donors required for *de novo* purine synthesis.

**Keywords:** Acetazolamide, BrdU incorporation, carbonic anhydrase inhibition, cell cycle arrest, *de novo* purine biosynthesis

## Introduction

Rapid cell proliferation demands a continuous and abundant supply of purine nucleotides to sustain DNA replication, RNA synthesis, and energy-dependent signaling. To meet these biosynthetic requirements, proliferating cells upregulate purine production primarily through the *de novo* synthesis pathway, which assembles the purine ring from small-molecule precursors including amino acids,  $\text{CO}_2$ , and bicarbonate ( $\text{HCO}_3^-$ ) [1,2]. The dependence of proliferating cells on *de novo* purine synthesis is especially pronounced in T lymphocytes, where mitogenic activation triggers a dramatic

metabolic reprogramming that elevates nucleotide biosynthesis to fuel clonal expansion [3,4]. This metabolic vulnerability has long been recognized as a clinically actionable target: antifolate agents such as methotrexate exert their immunosuppressive and antiproliferative effects primarily by blocking the folate-dependent formylation steps (steps 3 and 9) of *de novo* purine synthesis, thereby depleting the nucleotide pools required for S phase entry and cell division [5,6].

The ten-step *de novo* purine synthesis pathway converts phosphoribosyl pyrophosphate (PRPP) to inosine 5'-monophosphate (IMP) through

sequential enzymatic reactions occurring in the cytosol [1]. Among these, the bifunctional enzyme phosphoribosylaminoimidazole carboxylase/phosphoribosylaminoimidazolesuccinocarboxamide synthetase (PAICS) catalyzes the sixth step, the carboxylation of 5-aminoimidazole ribonucleotide (AIR) to 4-carboxy-5-aminoimidazole ribonucleotide (CAIR), a reaction that uniquely requires  $\text{CO}_2/\text{HCO}_3^-$  as the direct carboxyl donor [7,8]. Unlike the folate-dependent formylation steps, this carboxylation step is governed strictly by the intracellular availability of dissolved  $\text{CO}_2$  and bicarbonate. Recent evidence further demonstrates that *de novo* purine biosynthesis is cell cycle-regulated, with peak pathway flux occurring in G1 phase when cells accumulate the nucleotide pools necessary for S phase DNA replication, an activity that correlates with the assembly of supramolecular purinosome complexes [9]. Despite the recognized importance of this carboxylation node, it has remained largely unexplored as a pharmacological target for antiproliferative intervention.

The intracellular  $\text{CO}_2/\text{HCO}_3^-$  equilibrium, and hence the availability of carboxyl donors for PAICS, is dynamically regulated by carbonic anhydrase (CA), a family of zinc metalloenzymes that catalyze the reversible hydration of  $\text{CO}_2$  to  $\text{HCO}_3^-$  and a proton [10]. Fifteen catalytically active human CA isoforms are known, with distinct subcellular localizations spanning the cytosol (CA I, CA II, CA III), mitochondria (CA VA, CA VB), and plasma membrane (CA IX, CA XII, among others) [10,11]. The cytosolic isoforms, particularly CA II, are the primary regulators of intracellular  $\text{CO}_2/\text{HCO}_3^-$  homeostasis and are potently inhibited by acetazolamide, a sulfonamide-class inhibitor with nanomolar affinity for CA II ( $K_i = 12$  nM) [11]. Beyond their classical roles in acid-base balance and fluid secretion, CA inhibitors have attracted increasing interest as antiproliferative agents. Pharmacological inhibition of CA XII in T-cell lymphoma cell lines was reported to reduce cell proliferation and induce apoptosis [12], providing direct precedent for a role of CA-dependent regulation in lymphocyte biology. These observations raise the possibility that CA-

mediated  $\text{CO}_2/\text{HCO}_3^-$  homeostasis may represent a broader regulatory mechanism in proliferating immune cells, potentially through its influence on *de novo* purine biosynthesis.

The pivotal role of *de novo* purine synthesis in T lymphocyte proliferation has been well established. Activated T lymphocytes depend critically on this pathway for clonal expansion, with purines specifically governing G1-to-S phase transition and S phase progression [3]. Disruption of purine biosynthesis, whether through antifolate agents, IMPDH inhibitors, or nucleotide pool depletion, consistently produces G1/S cell cycle arrest in mitogen-stimulated lymphocytes [3,5,6]. Prior work from our laboratory established that disrupting carboxylation reactions in purine biosynthesis through biotin sequestration by avidin effectively suppresses PHA-induced PBMC proliferation [13], providing proof-of-concept that the carboxylation node is a functionally critical control point. Building on this finding, we reasoned that an alternative strategy to limit carboxyl donor availability, specifically by inhibiting CA-mediated  $\text{CO}_2/\text{HCO}_3^-$  interconversion, should produce comparable antiproliferative effects by impairing the PAICS-catalyzed step in purine biosynthesis.

The present study was therefore designed to test this hypothesis by evaluating the effects of acetazolamide on cell viability, DNA synthesis, and cell cycle distribution in human peripheral blood mononuclear cells (PBMCs) stimulated with phytohemagglutinin (PHA) or interleukin-2 (IL-2), two mechanistically distinct mitogens that activate T lymphocyte proliferation through lectin-mediated TCR crosslinking and cytokine receptor signaling, respectively [14,15]. We hypothesized that acetazolamide-mediated CA inhibition would impair *de novo* purine synthesis at the carboxylation step, deplete nucleotide pools, arrest cells at the G1/S checkpoint, and suppress overall proliferative activity. To our knowledge, this is the first study to systematically investigate the antiproliferative potential of CA inhibition through the lens of *de novo* purine biosynthesis disruption in primary human lymphocytes.

## Methods

### Ethical approval and blood sample collection

This study was conducted at the Department of Biochemistry and Molecular Biology, Department of Medical Biology, and Department of Clinical Pathology, Faculty of Medicine, Universitas Indonesia, Jakarta, from March 2015 to March 2016. The study protocol was approved by the Medical Ethics Committee of the Faculty of Medicine, Universitas Indonesia (approval number: 662/UN2.F1/ETIK/2015). All procedures were performed in accordance with the Declaration of Helsinki. Peripheral blood samples were collected from nine healthy adult volunteers after obtaining written informed consent. Approximately 10 mL of venous blood was drawn from each donor into heparinized vacutainer tubes and processed within 2 hours of collection.

### PBMC isolation

PBMCs were isolated by density gradient centrifugation as described by Bøyum [16]. Briefly, 3 mL of Ficoll-Paque Plus (GE Healthcare, Little Chalfont, UK) was layered into a sterile 15 mL conical centrifuge tube. Four milliliters of blood diluted 1:1 with phosphate-buffered saline (PBS, pH 7.4; Sigma-Aldrich, St. Louis, MO, USA) was gently overlaid onto the Ficoll-Paque to preserve the density gradient interface. Tubes were centrifuged at  $400 \times g$  for 30 minutes at 18–20°C with the centrifuge brake disengaged. The buffy coat at the plasma-Ficoll interface was carefully aspirated and transferred to a new tube. Cells were washed twice with PBS by centrifugation at  $300 \times g$  for 10 minutes at room temperature. The resulting cell pellet was resuspended in complete RPMI-1640 medium (Lonza, Basel, Switzerland) supplemented with 10% heat-inactivated fetal bovine serum (FBS; Gibco, Thermo Fisher Scientific, Waltham, MA, USA), 100 U/mL penicillin, and 100 µg/mL streptomycin (Gibco, Thermo Fisher Scientific). Cell density and viability were determined by trypan blue exclusion using a hemocytometer. Only cell suspensions with viability exceeding 95% were used in subsequent experiments.

### Cell culture and mitogenic stimulation

PBMCs were seeded in 96-well flat-bottom plates (Corning, Corning, NY, USA) at a density of  $1.5 \times 10^5$  cells per well in 200 µL of complete RPMI-1640 medium. Cells were stimulated with either phytohemagglutinin (PHA; 1% v/v; Gibco, Thermo Fisher Scientific, Waltham, MA, USA) [14] or recombinant human interleukin-2 (IL-2; 10 ng/mL; PeproTech, Rocky Hill, NJ, USA) [15] to induce T lymphocyte proliferation. Acetazolamide (Sigma-Aldrich, St. Louis, MO, USA) was dissolved in dimethyl sulfoxide (DMSO; Sigma-Aldrich) to prepare a 50 mM stock solution stored at -20°C, and further diluted in complete medium to final concentrations of 6.25, 12.5, 25, and 50 µM. Acetazolamide was added simultaneously with mitogens at the start of culture. The final DMSO concentration did not exceed 0.1% (v/v) in any well. Control groups received an equivalent volume of DMSO vehicle without acetazolamide. Unstimulated PBMCs cultured in complete medium served as the negative control. All cultures were maintained at 37°C in a humidified incubator with 5% CO<sub>2</sub> for 72 hours prior to analysis. All experimental conditions were performed in triplicate.

### Cell viability assay

Cell viability was assessed using the WST-1 colorimetric assay (WST-1 Cell Proliferation Reagent; Roche Diagnostics, Mannheim, Germany), which measures the metabolic activity of mitochondrial dehydrogenases in viable cells [17]. After 72 hours of culture, 10 µL of WST-1 reagent was added directly to each well containing 100 µL of cell suspension. Plates were incubated for 2 hours at 37°C in 5% CO<sub>2</sub> to allow formazan product formation. After gentle mixing on a microplate shaker, absorbance was measured at 450 nm with a reference wavelength of 650 nm using a microplate spectrophotometer (Multiskan GO; Thermo Fisher Scientific, Waltham, MA, USA). Cell viability was expressed as a percentage relative to the DMSO vehicle control: Viability (%) =  $(OD_{\sim\text{treated}\sim} / OD_{\sim\text{control}\sim}) \times 100$ . Data are presented as mean  $\pm$  standard deviation (SD) from three independent

experiments each performed with PBMCs from a different donor.

### DNA synthesis assay

Active DNA synthesis was quantified by 5-bromo-2'-deoxyuridine (BrdU) incorporation into newly replicated DNA using the Cell Proliferation ELISA BrdU colorimetric kit (Roche Diagnostics, Mannheim, Germany), as a validated non-radioactive alternative to [<sup>3</sup>H]-thymidine incorporation [18]. At 70 hours of culture, BrdU labeling solution was added to each well at a final concentration of 10 μM. Cells were pulse-labeled for 2 hours at 37°C. Following the labeling period, the plate was centrifuged at 300 × g for 10 minutes, the supernatant was discarded, and cells were fixed and DNA denatured with FixDenat solution (provided in the kit) for 30 minutes at room temperature. Anti-BrdU peroxidase-conjugated antibody (provided in the kit; diluted 1:100 in antibody dilution buffer) was added at 100 μL per well and incubated for 90 minutes at room temperature. Wells were washed three times with wash buffer. Substrate solution (tetramethylbenzidine; provided in the kit) was added at 100 μL per well and the colorimetric reaction was allowed to develop for 15–30 minutes at room temperature. The reaction was terminated by addition of 25 μL of 1 M H<sub>2</sub>SO<sub>4</sub> and absorbance was measured at 450 nm with a reference wavelength of 690 nm within 5 minutes of stopping the reaction. BrdU incorporation, directly reflecting the rate of DNA synthesis, was proportional to absorbance. Results are expressed as mean ± SD from three independent experiments.

### Cell cycle analysis

Cell cycle distribution was determined by flow cytometric analysis of propidium iodide (PI)-stained cells following established protocols [19,20]. After 72 hours of culture, cells were harvested by centrifugation at 300 × g for 10 minutes, washed twice with cold PBS, and fixed in ice-cold 70% ethanol (Merck, Darmstadt, Germany) for a minimum of 2 hours at 4°C. Fixed cells

were washed with PBS to remove ethanol, then resuspended in 500 μL of PI staining solution containing 50 μg/mL propidium iodide (Sigma-Aldrich, St. Louis, MO, USA), 0.1 mg/mL RNase A (Sigma-Aldrich), and 0.05% (v/v) Triton X-100 (Sigma-Aldrich) in PBS. Samples were incubated for 30 minutes at 37°C in the dark to allow complete RNA digestion and stoichiometric DNA staining. Flow cytometric acquisition was performed on a FACSCalibur instrument (BD Biosciences, San Jose, CA, USA), with PI fluorescence detected using 488 nm laser excitation and a 617 nm bandpass emission filter. A minimum of 10,000 events were acquired per sample. The percentage of cells in G<sub>0</sub>/G<sub>1</sub>, S, and G<sub>2</sub>/M phases was determined from DNA content frequency histograms using ModFit LT software version 4.0 (Verity Software House, Topsham, ME, USA).

### Statistical analysis

All assays were performed in triplicate wells and each experiment was independently repeated at least three times using PBMCs from different donors. Data are presented as mean ± SD. Statistical comparisons were performed using one-way analysis of variance (ANOVA) followed by Tukey's post hoc test for multiple comparisons, implemented in GraphPad Prism version 10.0 (GraphPad Software, San Diego, CA, USA). A p-value of less than 0.05 was considered statistically significant.

## Results

### Optimization of mitogenic stimulation conditions

To determine the optimal conditions for assessing acetazolamide effects on PBMC proliferation, preliminary experiments were conducted to establish the most effective concentrations and timing for mitogenic stimulation. PBMCs were cultured with varying concentrations of PHA (0.5%, 1%, and 2% v/v) or IL-2 (5, 10, and 20 ng/mL), and cell responses were evaluated at 24, 48, and 72 hours post-stimulation using the WST-1 viability assay and BrdU incorporation assay.

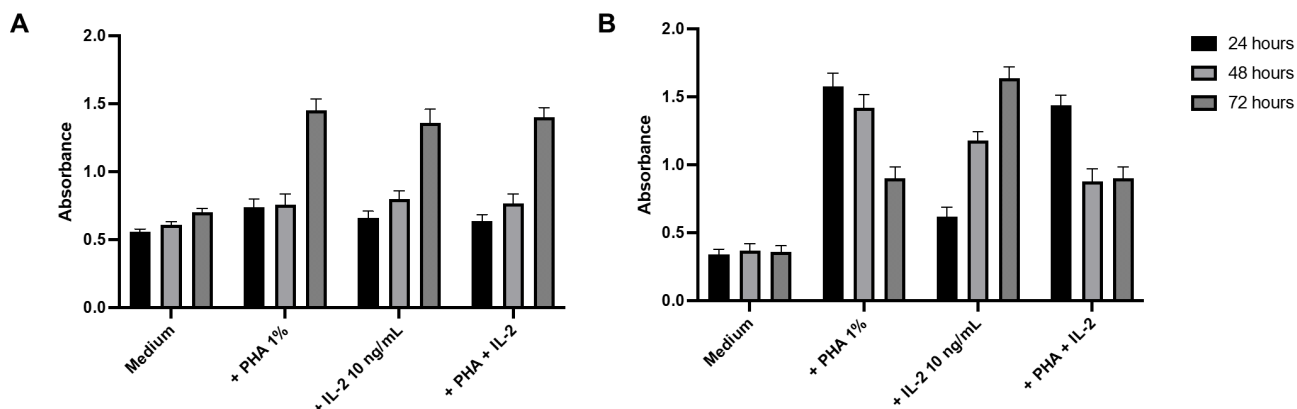


**Figure 1. Time-dependent effects of PHA and IL-2 on PBMC viability and DNA synthesis.** PBMCs were stimulated with 1% (v/v) PHA or 10 ng/mL IL-2 and harvested at 24, 48, and 72 hours. **(A)** Cell viability assessed using the WST-1 colorimetric assay; the tetrazolium salt WST-1 is cleaved by mitochondrial dehydrogenases in viable cells to produce a soluble formazan product, measured at 450 nm (reference wavelength: 650 nm). Both mitogens induced maximum PBMC viability at 72 hours. **(B)** DNA synthesis quantified by BrdU incorporation assay; after pulse-labeling, incorporated BrdU was detected using an anti-BrdU peroxidase-conjugated antibody, with absorbance measured at 450 nm (reference wavelength: 690 nm). PHA stimulation resulted in peak DNA synthesis at 24 hours, while IL-2 stimulation induced maximum DNA synthesis at 72 hours. Data in both panels represent mean  $\pm$  SD from three independent experiments performed in triplicate.

The results demonstrated that 1% (v/v) PHA and 10 ng/mL IL-2 produced maximum PBMC viability and proliferation. Time course analysis revealed that PBMC viability peaked at 72 hours for both PHA and IL-2 stimulation (Figure 1A). However, the kinetics of DNA synthesis differed between the two mitogens: PHA-stimulated PBMCs exhibited maximum DNA synthesis at 24 hours post-stimulation, whereas IL-2-stimulated PBMCs showed peak DNA synthesis at 72 hours (Figure 1B). Based on these optimization experiments, subsequent acetazolamide treatment studies were performed using 1% PHA or 10 ng/mL IL-2 with the respective optimal incubation times.

### Effects of acetazolamide on PBMC viability

To investigate whether carbonic anhydrase inhibition affects PBMC survival, cells were stimulated with either 1% PHA or 10 ng/mL IL-2 in the presence or absence of varying concentrations of acetazolamide (6.25, 12.5, 25, and 50  $\mu$ M). Cell viability was assessed at 24, 48, and 72 hours using the WST-1 assay.

Acetazolamide treatment significantly reduced PBMC viability in a dose-dependent manner in both PHA-stimulated and IL-2-stimulated cultures (Figure 2). At the highest concentration tested (50

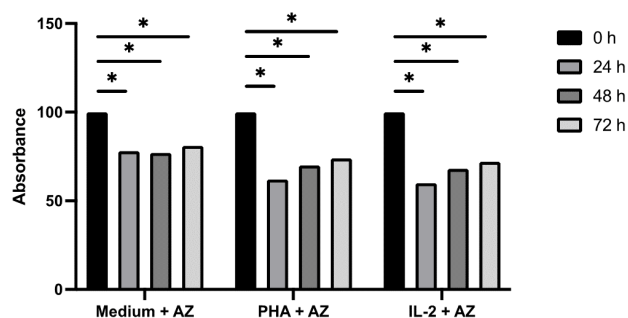


**Figure 2. Dose-dependent effect of acetazolamide on the viability of mitogen-stimulated PBMCs.** PBMCs were stimulated with 1% (v/v) PHA (panel A) or 10 ng/mL IL-2 (panel B) in the presence of increasing concentrations of acetazolamide (0, 6.25, 12.5, 25, and 50  $\mu$ M). Cell viability was evaluated at 72 hours using the WST-1 assay and expressed as percentage relative to vehicle-treated control cells (set as 100%). Data represent mean  $\pm$  SD from three independent experiments performed in triplicate. Asterisks indicate statistically significant differences compared to control (\*  $p < 0.05$ , one-way ANOVA followed by Tukey's post hoc test).

$\mu$ M), acetazolamide caused significant decreases in cell viability at all time points examined: 24 hours ( $p < 0.05$ ), 48 hours ( $p < 0.05$ ), and 72 hours ( $p < 0.05$ ) compared to vehicle-treated controls. At 72 hours, 50  $\mu$ M acetazolamide reduced viability to approximately 60% and 55% of control levels in PHA-stimulated and IL-2-stimulated cultures, respectively, indicating that carbonic anhydrase inhibition compromises mitochondrial metabolic activity in proliferating PBMCs.

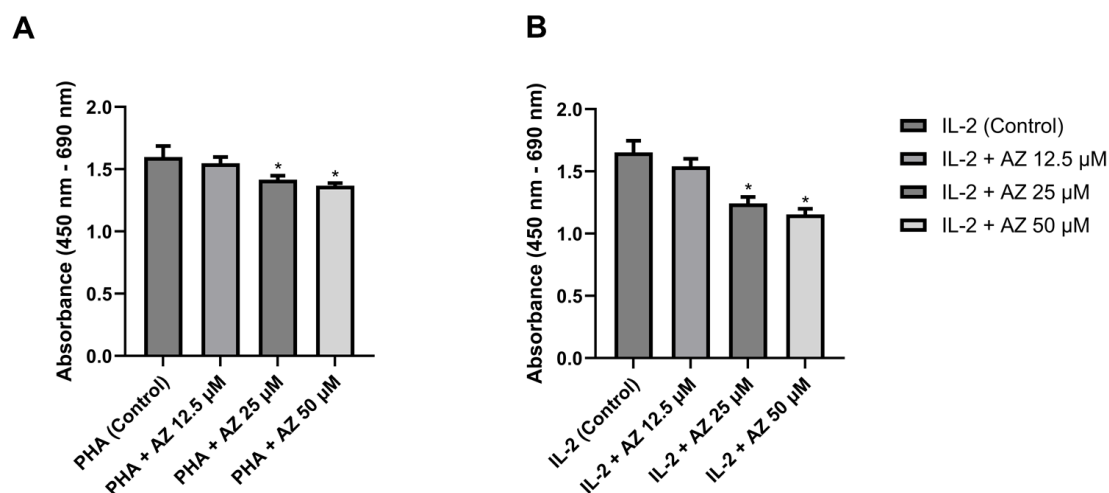


**Figure 3. Dose-dependent inhibition of DNA synthesis by acetazolamide in mitogen-stimulated PBMCs.** (A) PBMCs stimulated with 1% (v/v) PHA in the presence of increasing concentrations of acetazolamide (0, 6.25, 12.5, 25, and 50  $\mu\text{M}$ ). DNA synthesis was quantified by BrdU incorporation assay at 24 hours post-stimulation; absorbance at 450 nm (reference wavelength: 690 nm) is directly proportional to the amount of BrdU incorporated into newly synthesized DNA. Significant inhibition was first observed at 25  $\mu\text{M}$  and higher concentrations. (B) PBMCs stimulated with 10 ng/mL IL-2 in the presence of the same acetazolamide concentration range, with BrdU incorporation assessed at 72 hours post-stimulation. IL-2-stimulated PBMCs exhibited greater sensitivity to acetazolamide than PHA-stimulated cells, with significant inhibition observed at 12.5  $\mu\text{M}$  and higher concentrations. Data in both panels are expressed as percentage relative to vehicle-treated control and represent mean  $\pm$  SD from three independent experiments performed in triplicate. Asterisks indicate statistically significant differences compared to control (\*  $p < 0.05$ , one-way ANOVA followed by Tukey's post hoc test).

### Effects of acetazolamide on DNA synthesis

To determine whether acetazolamide-mediated reduction in cell viability was associated with impaired DNA synthesis, BrdU incorporation was measured in PBMCs stimulated with PHA or IL-2 in the presence of various acetazolamide concentrations. Based on the time course data showing optimal DNA synthesis (Figure 1B), BrdU incorporation was assessed at 24 hours for PHA-stimulated cultures and at 72 hours for IL-2-stimulated cultures.

Acetazolamide treatment resulted in significant, dose-dependent inhibition of DNA synthesis in both PHA-stimulated and IL-2-stimulated PBMCs (Figure 3). IL-2-stimulated cells exhibited greater sensitivity to acetazolamide than PHA-stimulated cells. In PHA-stimulated cultures, significant inhibition of DNA synthesis was observed at concentrations of 25  $\mu\text{M}$  and above ( $p < 0.05$ ) (Figure 3A). In contrast, IL-2-stimulated PBMCs showed significant reduction in BrdU incorporation at the lower concentration of 12.5  $\mu\text{M}$  ( $p < 0.05$ ) (Figure 3B). At 50  $\mu\text{M}$  acetazolamide, DNA synthesis was reduced to approximately 45% and 30% of control levels

in PHA-stimulated and IL-2-stimulated cultures, respectively, indicating potent suppression of DNA replication.

### Effects of acetazolamide on cell cycle progression

To elucidate the mechanism underlying acetazolamide-mediated inhibition of PBMC proliferation, cell cycle distribution was analyzed by flow cytometry using propidium iodide staining. PBMCs were cultured for 72 hours with or without mitogenic stimulation (1% PHA or 10 ng/mL IL-2) in the presence or absence of 50  $\mu\text{M}$  acetazolamide.

Flow cytometric analysis revealed distinct cell cycle profiles among the experimental groups (Table 1, Figure 4). Unstimulated control PBMCs remained predominantly in the G0/G1 phase (92.77%), with minimal cells in S phase (1.07%) or G2/M phase (6.16%), confirming their quiescent state (Figure 4A). Mitogenic stimulation with PHA or IL-2 induced cell cycle progression, as evidenced by increased proportions of cells entering S phase. PHA stimulation was more potent than IL-2, increasing the S phase population from 1.07%

**Table 1.** Cell cycle distribution of PBMCs under different culture conditions

Condition	Control group			Treatment group (added 50 $\mu$ M AZ)		
	G1 phase (%)	S phase (%)	G2 phase (%)	G1 phase (%)	S phase (%)	G2 phase (%)
Unstimulated PBMC	99.73	0.27	0	99.43	0	0.57
PHA-stimulated PBMC	91.48	8.52	0	96.18	3.82	0.57
IL-2-stimulated PBMC	98.40	1.27	0.33	100.00	0	0

(unstimulated) to 8.52%, while IL-2 stimulation resulted in a more modest increase to 1.27% (Table 1, Figure 4B and 4C, left panels).

Treatment with 50  $\mu$ M acetazolamide markedly inhibited cell cycle progression in both PHA-stimulated and IL-2-stimulated cultures. In PHA-stimulated PBMCs, acetazolamide reduced the S phase population from 8.52% to 3.82%, representing a 55% reduction, while the G0/G1 fraction correspondingly increased from 91.48% to 96.18% (Figure 4B, right panel). The effect was even more pronounced in IL-2-stimulated cultures, where acetazolamide completely abolished S phase entry, reducing the S phase fraction from 1.27% to 0% and driving the G0/G1 fraction to 100% (Figure 4C, right panel). These findings indicate potent G1/S arrest in both mitogen-activated cell populations.

Notably, across all acetazolamide-treated groups, the G2/M fraction was consistently suppressed to  $\leq 0.57\%$ , regardless of the mitogenic stimulus applied (Table 1). This uniform near-absence of G2/M cells in acetazolamide-treated cultures, including in PHA-stimulated cells where robust G2/M entry would otherwise be expected, provides additional evidence that acetazolamide arrests cells at the G1/S transition, preventing any progression to subsequent cell cycle phases. The convergence of G2/M values across treated groups further supports a specific blockade at the G1/S checkpoint rather than a non-specific cytostatic effect.

Taken together, these results demonstrate that acetazolamide effectively blocks PBMC progression from G0/G1 phase into S phase, preventing DNA synthesis and cell division in a manner consistent with disruption of the nucleotide pool required for S phase entry.

## Discussion

The principal finding of this study is that pharmacological inhibition of carbonic anhydrase by acetazolamide suppresses human PBMC proliferation through a coordinated set of effects: reduced cell viability, dose-dependent inhibition of DNA synthesis, and arrest of cell cycle progression at the G1/S transition. These effects were observed consistently across two independent mitogenic stimulation systems, PHA and IL-2, and were dose-dependent, suggesting that CA activity is required to sustain the proliferative response of activated T lymphocytes. To our knowledge, this is the first report demonstrating that targeting carbonic anhydrase pharmacologically is sufficient to halt lymphocyte proliferation, and the pattern of effects observed is consistent with a mechanism involving disruption of  $\text{CO}_2/\text{HCO}_3^-$ -dependent carboxylation in *de novo* purine biosynthesis.

The *de novo* purine synthesis pathway requires  $\text{CO}_2$  as a critical substrate for completing the purine ring structure. A pivotal step in this pathway is the carboxylation of 5-phosphoribosyl-5-aminoimidazole (AIR) to 5-phosphoribosyl-4-carboxy-5-aminoimidazole (CAIR), catalyzed by phosphoribosylaminoimidazole carboxylase (AIR carboxylase). This reaction constitutes the sixth of ten sequential steps and utilizes  $\text{CO}_2/\text{HCO}_3^-$  as the carboxyl donor [7]. The intracellular concentration of  $\text{CO}_2$  and its hydrated form, bicarbonate ( $\text{HCO}_3^-$ ), is maintained by carbonic anhydrase (CA), which catalyzes the reversible interconversion of  $\text{CO}_2$  and  $\text{HCO}_3^-$  and thereby regulates the availability of carboxyl donors for biosynthetic reactions [10]. This regulatory function positions CA as a potential control point for modulating *de novo* purine synthesis and, consequently, cell proliferation. Consistent

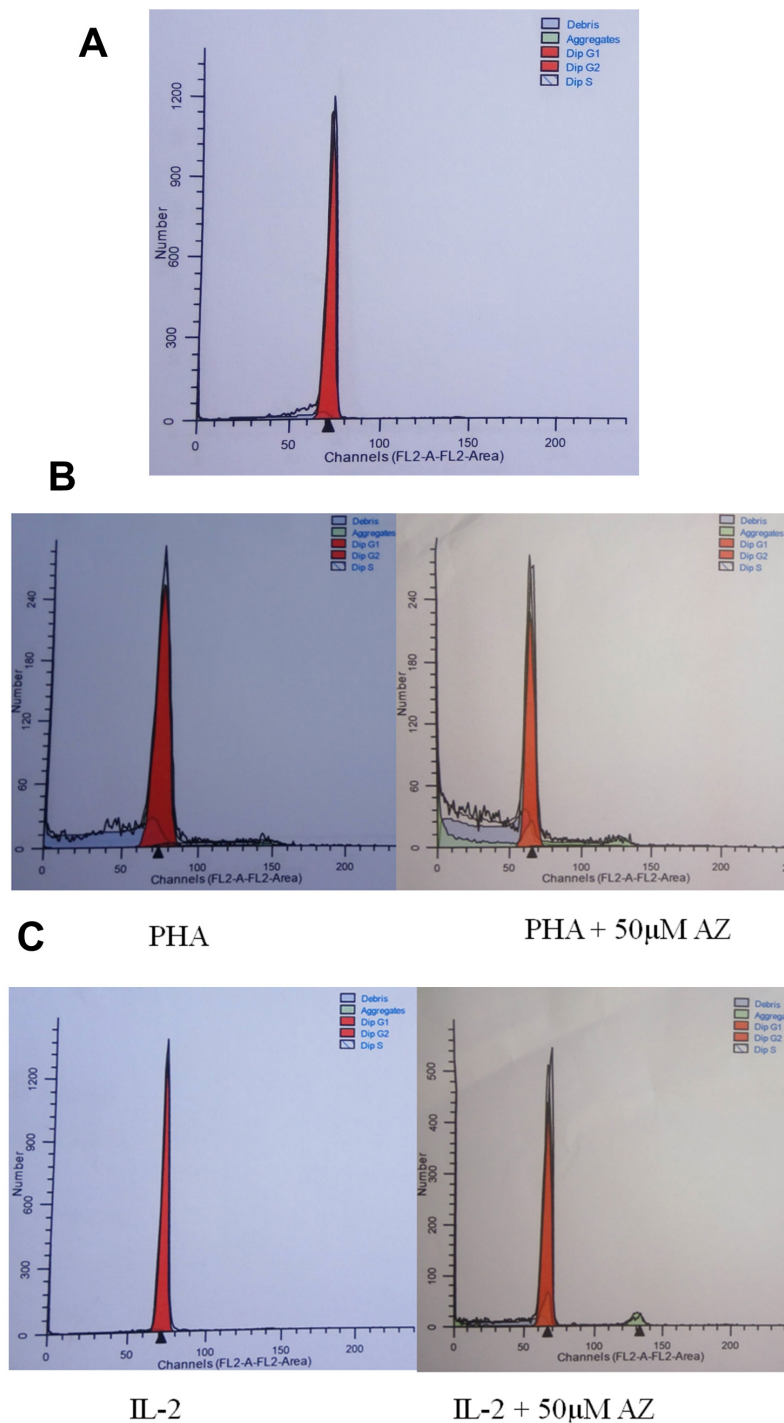


**Figure 4. Effect of acetazolamide on cell cycle distribution in unstimulated and mitogen-stimulated PBMCs.** Representative flow cytometry histograms showing DNA content distribution (propidium iodide staining) after 72 hours of culture. Cell cycle analysis was performed using a FACSCalibur flow cytometer (BD Biosciences, San Jose, CA, USA) and ModFit LT software version 4 (Verity Software House, Topsham, ME, USA). **(A)** Unstimulated PBMCs cultured in complete RPMI-1640 medium without mitogenic stimulation. The majority of cells (92.77%) remained in G0/G1 phase, reflecting the quiescent state of resting lymphocytes, with minimal S phase (1.07%) and G2/M phase (6.16%) populations. **(B)** PHA-stimulated PBMCs (1% v/v PHA). Left panel: increased S phase population (8.52%) reflecting active cell cycle progression. Right panel: treatment with 50  $\mu$ M acetazolamide reduced S phase entry to 3.82% with a corresponding increase in the G0/G1 fraction (96.18%) and G2/M suppressed to 0.57%, demonstrating G1/S arrest. **(C)** IL-2-stimulated PBMCs (10 ng/mL). Left panel: modest increase in S phase population (1.27%). Right panel: treatment with 50  $\mu$ M acetazolamide completely abolished S phase entry (0%), with a G0/G1 fraction of 100% and no detectable G2/M population, indicating complete G1/S cell cycle arrest. Data represent mean values from three independent experiments. G2/M fractions across all acetazolamide-treated groups were uniformly suppressed to  $\leq$ 0.57%, consistent with specific arrest at the G1/S transition.

with this view, recent evidence demonstrates that the assembly of the purinosome — a dynamic multienzyme complex that channels substrates through the *de novo* purine pathway — is itself sensitive to intracellular metabolic conditions, including changes in  $\text{CO}_2/\text{HCO}_3^-$  availability and oxygen tension [21], underscoring the susceptibility of this biosynthetic machinery to perturbations in carbonic anhydrase activity. More broadly, blockade of *de novo* nucleoside phosphate synthesis has been recognized as a critical checkpoint controlling T lymphocyte proliferation in diverse immunological contexts, including immune checkpoint signaling mediated by PD-L1 [22], further situating CA-dependent  $\text{CO}_2/\text{HCO}_3^-$  regulation within a wider network of metabolic control over immune cell expansion.

In the present study, we employed the WST-1 assay to assess cell viability as an indirect index of overall mitochondrial metabolic activity. Acetazolamide significantly reduced the viability of mitogen-stimulated PBMCs in a dose-dependent manner, with 50  $\mu\text{M}$  acetazolamide reducing viability to approximately 60% and 55% of control in PHA- and IL-2-stimulated cultures, respectively. The reduction in WST-1 conversion is consistent with a diminished number of metabolically active, proliferating cells, most likely reflecting cell cycle arrest rather than frank cytotoxicity, an interpretation supported by the cell cycle data discussed below. It should be noted, however, that the WST-1 assay does not discriminate between cytostatic and cytotoxic effects; thus, a contribution of reduced metabolic activity per cell cannot be entirely excluded and warrants investigation in future studies using orthogonal viability measures such as Trypan blue exclusion or Annexin V staining.

Direct quantification of DNA synthesis by BrdU incorporation provided more specific evidence for an antiproliferative effect. Acetazolamide treatment produced significant, dose-dependent suppression of BrdU incorporation in both PHA-stimulated and IL-2-stimulated PBMCs [18]. IL-2-stimulated cells exhibited greater sensitivity to acetazolamide, with significant inhibition

occurring at 12.5  $\mu\text{M}$  compared to 25  $\mu\text{M}$  in PHA-stimulated cells. This differential sensitivity may reflect the distinct signaling and metabolic demands of the two mitogenic pathways: PHA activates a broad, lectin-mediated polyclonal T cell response with high baseline proliferative capacity, whereas IL-2 drives a more selective cytokine-dependent proliferation that may be more acutely dependent on *de novo* purine synthesis [9]. T cell activation in general entails extensive metabolic reprogramming — encompassing elevated rates of protein synthesis, anabolic biosynthesis, and energy production — that renders proliferating lymphocytes uniquely dependent on the integrated operation of biosynthetic pathways, including nucleotide synthesis [23]. The convergence of reduced WST-1 activity and suppressed BrdU incorporation across both stimulation conditions supports the conclusion that acetazolamide impairs active cell division rather than exclusively affecting metabolic activity in non-dividing cells.

Flow cytometric analysis of cell cycle distribution provided mechanistic insight into the antiproliferative effects of acetazolamide. Acetazolamide treatment arrested cells in the G<sub>0</sub>/G<sub>1</sub> phase, preventing progression into S phase [19,20]. In PHA-stimulated cultures, the S phase population decreased from 8.52% to 3.82%, while in IL-2-stimulated cultures, S phase entry was completely abolished (from 1.27% to 0%). Correspondingly, a consistent feature across all acetazolamide-treated groups was the suppression of the G<sub>2</sub>/M fraction to  $\leq 0.57\%$ , regardless of the mitogenic stimulus applied. This uniform near-absence of G<sub>2</sub>/M cells in treated cultures, including in PHA-stimulated cells where active cycling would be expected without treatment, is consistent with a block specifically at the G<sub>1</sub>/S transition that prevents cells from advancing to G<sub>2</sub>/M. This pattern strengthens the inference of a G<sub>1</sub>/S checkpoint arrest rather than a non-specific reduction in overall cellular activity. The observed G<sub>1</sub>/S arrest is consistent with insufficient nucleotide availability, as nucleotide synthesis increases dramatically in late G<sub>1</sub> phase to provide the substrate pool required for imminent DNA replication in S phase [3,4].

The requirement for adequate nucleotide pools at the G1/S checkpoint is well established [3,4]. Interference with nucleotide production during this critical transition prevents cells from satisfying the threshold required for S phase commitment [5]. Our findings parallel those reported for classical purine synthesis inhibitors such as methotrexate and 5-fluorouracil, which also abolish IL-2-induced T cell division by disrupting nucleotide synthesis [9]. While these established antifolates target the formylation steps of *de novo* purine synthesis, the present study demonstrates that targeting the carboxylation step through CA inhibition produces a comparable antiproliferative outcome, pointing to an alternative and hitherto underexplored node of vulnerability within the same pathway.

To our knowledge, this is the first report demonstrating that pharmacological inhibition of carbonic anhydrase can effectively suppress cell proliferation through disruption of the carboxylation step in *de novo* purine synthesis in human primary lymphocytes. Previous work from our laboratory showed that depletion of biotin via avidin binding inhibits PHA-induced PBMC proliferation [13], providing proof of concept that carboxylation reactions represent critical control points in the purine biosynthetic pathway. The present study extends this finding by demonstrating that targeting the carboxyl donor supply, rather than the carboxylase cofactor, produces a similar antiproliferative outcome. It further identifies CA as an enzymatic regulator linking  $\text{CO}_2/\text{HCO}_3^-$  homeostasis to cell cycle progression. The dose-dependent nature of the acetazolamide effects and their selectivity for mitogen-activated, proliferating cells over quiescent unstimulated PBMCs suggest that rapidly dividing cells with high nucleotide demands are preferentially affected, a property of potential therapeutic relevance. CA inhibitors have received increasing attention as antiproliferative and anticancer agents over the past decade, and recent patent and literature analyses document a robust pipeline of CA-targeting compounds with demonstrated activity in diverse tumor models [24]. Notably, the CA inhibitor SLC-0111, a sulfonamide-

class agent with selectivity for tumor-associated CA IX, has entered Phase I clinical evaluation in patients with advanced solid tumors [25], providing direct translational validation that CA inhibition is a clinically actionable strategy and lending broader significance to the antiproliferative mechanism described in the present study.

Several limitations of the present study should be acknowledged. The proposed mechanism, namely that acetazolamide disrupts *de novo* purine synthesis via  $\text{CO}_2/\text{HCO}_3^-$  depletion at the AIR carboxylase step, is supported by the convergent phenotype of reduced DNA synthesis and G1/S arrest, but was not directly validated by measuring intracellular purine nucleotide pools or CA enzymatic activity under the experimental conditions used. Additionally, acetazolamide inhibits multiple CA isoforms with varying subcellular distributions [10], and the relative contribution of individual isoforms to the observed antiproliferative effects remains to be determined. Recent comprehensive analyses of isoform-specific CA inhibitor binding modes highlight that cytosolic isoforms (notably CA II) and tumor-associated transmembrane isoforms (CA IX, CA XII) can be differentially targeted through structural optimization [26], and future work employing isoform-selective inhibitors will be essential to dissect whether the antiproliferative effects observed here are predominantly mediated through cytosolic  $\text{CO}_2/\text{HCO}_3^-$  regulation or through additional mechanisms involving membrane-associated isoforms. Alternative mechanisms, including acetazolamide-mediated intracellular acidification and downstream effects on ceramide production and apoptosis as reported in CA IX-overexpressing tumor cells [12], cannot be excluded as contributing factors in the present system, particularly given the WST-1 reduction observed. Future studies employing rescue experiments with exogenous bicarbonate or purine supplementation, isoform-selective inhibitors, and direct metabolite profiling will be important to confirm the mechanistic model proposed here and to evaluate the potential therapeutic window for CA inhibition in proliferative diseases.

## Conclusion

This study demonstrates that pharmacological inhibition of carbonic anhydrase by acetazolamide significantly suppresses PBMC proliferation through convergent effects on cell viability, DNA synthesis, and cell cycle progression. Acetazolamide reduced WST-1-assessed cell viability and BrdU incorporation in a dose-dependent manner in both PHA- and IL-2-stimulated cultures, with IL-2-stimulated cells exhibiting greater sensitivity. Cell cycle analysis revealed consistent G1/S arrest across all acetazolamide-treated groups, manifested as increased G0/G1 retention, reduced S phase entry, and uniform suppression of G2/M populations to  $\leq 0.57\%$ , indicating that cells were blocked from advancing beyond the G1/S transition. These findings are consistent with a model in which CA inhibition disrupts intracellular  $\text{CO}_2/\text{HCO}_3^-$  homeostasis, limiting the carboxyl donor availability required for the AIR carboxylase-catalyzed step in *de novo* purine biosynthesis and thereby preventing cells from accumulating the nucleotide pools necessary for S phase entry. Together with prior evidence that biotin depletion, which similarly impairs carboxylation, inhibits lymphocyte proliferation [6], these results identify the carboxylation step in *de novo* purine synthesis as a previously underexplored antiproliferative target. The convergence of our findings with those obtained using classical antifolate agents underscores the therapeutic potential of targeting the purine biosynthetic pathway at the carboxylation node and warrants further investigation using direct mechanistic approaches in both normal and malignant proliferating cell systems.

## Acknowledgment

The authors gratefully acknowledge the support provided by the Department of Biochemistry and Molecular Biology, the Department of Medical Biology, and the Department of Clinical Pathology, Faculty of Medicine, Universitas Indonesia, for providing laboratory facilities and technical resources throughout the study. The authors also thank all healthy volunteers who generously donated blood samples for this research.

## Funding

Research study grant from Universitas Indonesia (*Hibah Penelitian Unggulan Perguruan Tinggi Universitas Indonesia*). Academic years 2014. No: 0958/H2.R12/HKP.05.00/2014.

## Declaration of interest

The authors declare no conflict of interest. The funders had no role in the design of the study; in the collection, analyses, or interpretation of data; in the writing of the manuscript; or in the decision to publish the results.

## Author contributions

SM: Conceptualization, Methodology, Investigation, Data Curation, Formal Analysis, Writing – Original Draft, Writing – Review & Editing, Project Administration. MS: Conceptualization, Methodology, Supervision, Funding Acquisition, Writing – Review & Editing. S: Formal Analysis, Writing – Original Draft, Writing – Review & Editing.

Received: September 17, 2025

Revised: February 10, 2026

Accepted: February 14, 2026

Published: February 16, 2026

## References

1. Lane AN, Fan TW-M. Regulation of mammalian nucleotide metabolism and biosynthesis. *Nucleic Acids Res.* 2015;43(4):2466-2485. <https://doi.org/10.1093/nar/gkv047>
2. Tran DH, Kim D, Kesavan R, Brown H, Dey T, Soflaee MH, et al. De novo and salvage purine synthesis pathways across tissues and tumors. *Cell.* 2024;187(13):3303-3318.e19. <https://doi.org/10.1016/j.cell.2024.04.004>
3. Quemeneur L, Gerland L-M, Flacher M, Ffrench M, Revillard J-P, Genestier L. Differential control of cell cycle, proliferation, and survival of primary T lymphocytes by purine and pyrimidine nucleotides. *J Immunol.* 2003;170(10):4986-4995. <https://doi.org/10.4049/jimmunol.170.10.4986>
4. Ali ES, Ben-Sahra I. Regulation of nucleotide metabolism in cancers and immune disorders. *Trends Cell Biol.* 2023;33(9):780-796. <https://doi.org/10.1016/j.tcb.2023.03.003>
5. Fairbanks LD, Ruckemann K, Qiu Y, Hawrylowicz CM, Richards DF, Swaminathan R, et al. Methotrexate inhibits

- the first committed step of purine biosynthesis in mitogen-stimulated human T-lymphocytes: a metabolic basis for efficacy in rheumatoid arthritis. *Biochem J.* 1999;342(Pt 1):143-152. <https://doi.org/10.1042/bj3420143>
6. Kondo M, Yamaoka T, Honda S, Miwa Y, Katashima R, Moritani M, et al. The rate of cell growth is regulated by purine biosynthesis via ATP production and G1 to S phase transition. *J Biochem.* 2000;128(1):57-64. <https://doi.org/10.1093/oxfordjournals.jbchem.a022730>
  7. Levenberg B, Buchanan JM. Biosynthesis of the purines. XII. Structure, enzymatic synthesis, and metabolism of 5-aminoimidazole ribotide. *J Biol Chem.* 1957;224(2):1005-1018. [https://doi.org/10.1016/S0021-9258\(18\)64992-0](https://doi.org/10.1016/S0021-9258(18)64992-0)
  8. Chegwiddden WR, Dodgson SJ, Spencer IM. The roles of carbonic anhydrase in metabolism, cell growth and cancer in animals. *EXS.* 2000;90:343-363. [https://doi.org/10.1007/978-3-0348-8446-4\\_16](https://doi.org/10.1007/978-3-0348-8446-4_16)
  9. Chan CY, Pedley AM, Kim D, Buber C, Zhao H, Bhatt M, et al. Purinosome formation as a function of the cell cycle. *Proc Natl Acad Sci USA.* 2015;112(5):1368-1373. <https://doi.org/10.1073/pnas.1423009112>
  10. Supuran CT. Carbonic anhydrases: novel therapeutic applications for inhibitors and activators. *Nat Rev Drug Discov.* 2008;7(2):168-181. <https://doi.org/10.1038/nrd2467>
  11. Tsikas D. Acetazolamide and human carbonic anhydrases: retrospect, review and discussion of an intimate relationship. *J Enzyme Inhib Med Chem.* 2024;39(1):2291336. <https://doi.org/10.1080/14756366.2023.2291336>
  12. Lounnas N, Rosilio C, Nebout M, Mary D, Griessinger E, Neffati Z, et al. Pharmacological inhibition of carbonic anhydrase XII interferes with cell proliferation and induces cell apoptosis in T-cell lymphomas. *Cancer Lett.* 2013;333(1):76-88. <https://doi.org/10.1016/j.canlet.2013.01.015>
  13. Firakania C, Mansur IG, Jusman SWA, Sadikin M. Avidin inhibits PHA-induced human peripheral blood mononuclear cell (PBMC) proliferation. *Med J Indones.* 2016;25(1):19-24. <https://doi.org/10.13181/mji.v25i1.1264>
  14. Movafagh A, Ghanati K, Amami D, Mahdavi SM, Hashemi M, Abdolahi DZ. The structure biology and application of phytohemagglutinin (PHA) in phytomedicine: with special up-to-date references to lectins. *J Paramed Sci.* 2013;4(1):14-20.
  15. Fung MM, Rohwer F, McGuire KL. IL-2 activation of a PI3K-dependent STAT3 serine phosphorylation pathway in primary human T cells. *Cell Signal.* 2003;15(7):625-636. [https://doi.org/10.1016/S0898-6568\(03\)00003-2](https://doi.org/10.1016/S0898-6568(03)00003-2)
  16. Boyum A. Isolation of lymphocytes, granulocytes and macrophages. *Scand J Immunol.* 1976;5(Suppl 5):9-15. <https://doi.org/10.1111/j.1365-3083.1976.tb03851.x>
  17. Berridge MV, Herst PM, Tan AS. Tetrazolium dyes as tools in cell biology: new insights into their cellular reduction. *Biotechnol Annu Rev.* 2005;11:127-152. [https://doi.org/10.1016/S1387-2656\(05\)11004-7](https://doi.org/10.1016/S1387-2656(05)11004-7)
  18. Gercel-Taylor C, Wians FH, Wendel GD, Taylor DD. In vitro sensitivity of lymphocyte BrdU incorporation assay: a non-radioactive alternative for lymphocyte proliferation assays. *Clin Immunol Immunopathol.* 1997;82(2):176-179. <https://doi.org/10.1006/clin.1996.4307>
  19. Nunez R. DNA measurement and cell cycle analysis by flow cytometry. *Curr Issues Mol Biol.* 2001;3(3):67-70.
  20. Pozarowski P, Darzynkiewicz Z. Analysis of cell cycle by flow cytometry. *Methods Mol Biol.* 2004;281:301-311. <https://doi.org/10.1385/1-59259-811-0:301>
  21. Doigneaux C, Pedley AM, Mistry IN, Papayova M, Benkovic SJ, Tavassoli A. Hypoxia drives the assembly of the multienzyme purinosome complex. *J Biol Chem.* 2020;295(29):9551-9566. <https://doi.org/10.1074/jbc.RA119.012175>
  22. Sondergaard JN, Coquet JM, Ndhlovu LC, Godfrey DI, Bhatt DL, et al. Global alteration of T-lymphocyte metabolism by PD-L1 checkpoint involves a block of de novo nucleoside phosphate synthesis. *Cell Discov.* 2019;5:58. <https://doi.org/10.1038/s41421-019-0126-6>
  23. Marchingo JM, Cantrell DA. Protein synthesis, degradation, and energy metabolism in T cell immunity. *Cell Mol Immunol.* 2022;19(3):303-315. <https://doi.org/10.1038/s41423-021-00792-8>
  24. Nerella SG, Singh P, Arifuddin M, Supuran CT. Anticancer carbonic anhydrase inhibitors: a patent and literature update 2018-2022. *Expert Opin Ther Pat.* 2022;32(8):833-847. <https://doi.org/10.1080/13543776.2022.2083502>
  25. McDonald PC, Chia S, Bedard PL, Chu Q, Lyle M, Tang L, et al. A phase 1 study of SLC-0111, a novel inhibitor of carbonic anhydrase IX, in patients with advanced solid tumors. *Am J Clin Oncol.* 2020;43(7):484-490. <https://doi.org/10.1097/COC.0000000000000691>
  26. D'Ambrosio K, Di Fiore A, Alterio V, Langella E, Monti SM, Supuran CT, et al. Multiple binding modes of inhibitors to human carbonic anhydrases: an update on the design of isoform-specific modulators of activity. *Chem Rev.* 2025;125(1):150-222. <https://doi.org/10.1021/acs.chemrev.4c00586>